CONVERGENCE AND CONDITIONING OF DYNAMIC WAKE MODELS FOR FLIGHT DYNAMICS

Mong-che A. Hsieh
Graduate Research Assistant

David A. Peters
McDonnell Douglas Prof of Engineering

Department of Mechanical and Aerospace Engineering
Washington University in St. Louis
St. Louis, MO, USA

Abstract

The current limitations of the Morillo-Peters model for mass-source rotors is that the mass and damping matrices are ill conditioned at low frequencies. The ill conditioning, in turn, causes the solution to converge slowly. The ill conditioning and slow convergence may be attributed to the truncated mass and damping matrices which do not incorporate the logarithmic potential function due to a singularity. In order to try to improve the conditioning and convergence issue, we included the $m = n$ terms to the mass and damping matrices. In previous work, this term was not included in the mass matrix because we did not have a closed form representation for it. Presently we have derived the closed-form velocity potential for these lowest-order terms for all harmonics. For the zero harmonic, we have developed a way to deal with an infinite integral for each harmonic. By adding this term, we add an extra row and column to the mass and damping matrix, thus adding an extra mode into the system when we perform the eigenvalue analysis. We used this approximate solution and compared the mode shapes to the solutions without the infinite term to verify that the solution retains its original shape with the added row and column. Then we compare the frequency response of the system with the added row and column to Morillo-Peters model and the convolution integral.

Introduction

In 1980 Dale Pitt and David Peters (Ref. 1) developed a linear, unsteady theory that relates the transient rotor loads to the overall transient response of the rotor induced flow flied. The assumption of the Pitt-Peters model is based on unsteady potential flow theory with superposition of pressure, in which the velocity field is derived from superimposing the unsteady pressure and static pressure of the flow. Even though the Pitt-Peters model allows up to eight states using associated Legendre functions, only 3-state and 5-state modes for forward flight were investigated. Today, virtually every stability and handling quality application utilizes the Pitt-Peters model. However, the model is limited to the crudest wake description of uniform flow due to the limitation of the low-order approximation of the flow field. This model is not capable of providing a detailed description of the flow field, needed for thrust and moment analysis.

Due to the limitations of the Pitt-Peters model, David Peters and Chengjian He (Ref. 2) turned to a higher harmonic theory for the dynamic inflow in 1987. The pressure distribution for the Peters-He model was extended to include an arbitrary number of harmonics and radial functions for each harmonic, thus giving better correlation on the rotor disk plane than did the Pitt-Peters model. However, the limitation of the Peters-He model is that it can only analyze the normal component of the flow at the rotor disk, thus not being able to analyze all three components of the flow on and above the rotor plane.

Then in 2001, Jorge Morillo and David Peters (Ref. 3 and 4) addressed these issues by including an additional set of functions, which can, in turn, address the limitations of the Pitt-Peters and Peters-He model. Morillo expanded the pressure and velocity distribution (which uses Fourier series) to include both $n + m$ = even and $n + m$ = odd terms in the dynamic wake model. With the Morillo-Peters model, it was possible to obtain a good correlation with the exact solution from the convolution integral. Another advantage of the model is the ability to predict all three components of the flow field anywhere on or above the rotor disk plane. The only limitation to the Morillo-Peters model is that the fact that it could not treat non-zero flux mass sources. A disadvantage of the model is that the matrices are ill-conditioned, which causes the solution to converge slowly.

The latest addition to the dynamic wake model was to include the mass source terms. Ke Yu and David Peters (Ref. 5) developed an improved state-space representation to include non-zero flux mass source terms. The Yu-Peters model is derived using closed-form representations for the state-space representation, which can reduce the amount of computing time by eliminating the need to perform massive numerical inversions in dynamic simulation. However, the model still does not correct the ill-conditioning and exhibits slow convergence due to the omission of the infinite kinetic energy terms in the matrices.

In this present work, we intend to address the issue of ill-conditioning and slow convergence. Since previous work has been unsuccessful in

attempts to include the infinite kinetic energy term in the mass matrix, we address the issue by deriving an approximate solution. With the extra term, we add an extra row and column to the mass and damping matrix including the $n = m$ terms, hoping that this would help with the conditioning and convergence. Also, Morillo intended to examine the validity of using an On-Off formulation instead of the traditional Odd-Even formulation for further analysis. However, he did not delve further into this topic. Therefore, we would attempt to further derive the On-Off formulation with the added infinite term and determine whether this new formulation further improve the ill-conditioning of the matrices. Once we decide which formulation to adopt, we perform frequency response for non-zero frequencies and critical frequencies and compare this new model with the Morillo-Peters model. Since $m = 0$ is the most ill-conditioned case, we will concentrate on $m = 0$.

Nomenclature

$\hat{a}_n^m$	Cosine induced flow expansion coefficient
$\overline{a}_n^m$	Complex modulus of the induced flow expansion coefficient
$[D]$	Damping matrix
D_{jn}^{rm}	Element of [*D*]
H_n^m	Combination of double factorials, $\frac{(n+m-1)!!(n-m-1)!!}{(n+m)!!(n-m)!!}$
i	Imaginary value
j	Degree of Legendre function (polynomial number)
K_n^m	Legendre Constant, see Eqs. (24) and (25)
$[M]$	Mass matrix
M_{jn}^{rm}	Element of [*M*]
m	Order of Legendre function (harmonic number)
N	Highest subscript
n	Degree of Legendre function (polynomial number)
P_n^m	Associated Legendre functions of the first kind
$\overline{P}_n^m$	Normalized associated Legendre functions
Q_n^m	Associated Legendre functions of the second kind
$\overline{Q}_n^m$	Normalized associated Legendre functions
r	Order of Legendre function (harmonic number)
U_{nq}^m	Integral, see Eq. (14)
v	Induced velocity
α_n^m	Modes for Odd-Even formulation
γ, δ	On-Off modes for On-Off formulation
γ_n^m, δ_n^m	Induced inflow expansion coefficients for On-Off formulation
$\overline{v}$	Induced flow
Φ_n^{mc}	Pressure potential function
$\nu, \eta, \overline{\psi}$	Ellipsoidal coordinates
ξ, ξ_o	Stream wise variable
ρ_n^m	Normalized factor of associated Legendre function of the first kind
τ	Reduced time
τ_n^m	Pressure expansion coefficient
$\overline{\tau}_n^m$	Complex modulus of the pressure expansion coefficient
ω	Frequency

Superscripts and Subscripts

$(\ )^m$	Harmonic number
$(\ )_n$	Polynomial number
$(\ )_z$	Axial component
$(\ )_o$	$n + m = odd$ terms
$(\ )_e$	$n + m = even$ terms
$(\ )!!$	Double factorial, $n(n-2)(n-4)...2$ for n = *even* and $n(n-2)(n-4)...1$ for n = *odd*
$(\dot{\ })$	Derivative with respect to reduced time, i.e., $\partial / \partial \tau$

Infinite Solution (Hsieh-Peters Model) Analysis

As mentioned previously, the current disadvantage of the Morillo-Peters is that the matrices are ill conditioned. This may be due to the truncated mass and damping matrices. Yu and Peters studied the effect of including forcing terms that would yield the zero-order modes but with no zero-order terms in the basis functions. They found a very slow convergence in that case. For the purpose of this research, we derived an approximate value for the infinite integral in the mass matrix. This approximation approaches infinity in the proper way as the highest subscript N approaches infinity:

$$M_{00}^{00} = \left(\frac{4}{\pi^2} \sum_{n=1}^{N} \frac{1}{n} \right) + \frac{1}{2} \qquad \textbf{(1)}$$

There is no singularity for the damping matrix for these terms. Therefore, we can utilize the original formulation for the $m = n = 0$ term. By adding these extra terms, we add an extra row and column to the mass and stiffness matrix that includes the $n = m$ terms, as shown in the mass matrix in Eq. (2) indicated in bold and italicized.

$$\begin{bmatrix} \begin{bmatrix} M_{11}^{00} & M_{13}^{00} & M_{15}^{00} \\ M_{31}^{00} & M_{33}^{00} & M_{35}^{00} \\ M_{51}^{00} & M_{53}^{00} & M_{55}^{00} \end{bmatrix} & \begin{bmatrix} \boldsymbol{M_{10}^{00}} & M_{12}^{00} & M_{16}^{00} \\ \boldsymbol{M_{30}^{00}} & M_{32}^{00} & M_{34}^{00} \\ \boldsymbol{M_{50}^{00}} & M_{52}^{00} & M_{54}^{00} \end{bmatrix} \\ \begin{bmatrix} \boldsymbol{M_{01}^{00}} & \boldsymbol{M_{03}^{00}} & \boldsymbol{M_{05}^{00}} \\ M_{21}^{00} & M_{23}^{00} & M_{25}^{00} \\ M_{41}^{00} & M_{43}^{00} & M_{45}^{00} \end{bmatrix} & \begin{bmatrix} \boldsymbol{M_{00}^{00}} & \boldsymbol{M_{02}^{00}} & \boldsymbol{M_{04}^{00}} \\ \boldsymbol{M_{20}^{00}} & M_{22}^{00} & M_{24}^{00} \\ \boldsymbol{M_{40}^{00}} & M_{42}^{00} & M_{44}^{00} \end{bmatrix} \end{bmatrix} \quad \textbf{(2)}$$

The conditioning number of the matrices is the ratio of the highest eigenvalue to the lowest eigenvalue. Initial analysis of the conditioning of the mass and the damping matrix (shown in Figs. 1 and 2) indicates that the conditioning for both matrices did not improve significantly. Thus, contrary to our initial assumption, the new terms did not improve conditioning. However, it still could be that the new basis functions would improve convergence.

The next step is to determine how the new added row and column would affect the eigenvalue analysis of the system. In order to do so, we perform an eigenvalue analysis (Table 1) and compare the eigenvalues against the Morillo-Peters model. Since we added an extra row and column, we introduce an extra mode into the system. This extra mode represents the infinite kinetic energy solution, thus it has a very small eigenvalue. The remaining values remain within the same magnitude from the Morillo-Peters model. Based on this, one can conjecture that new eigenvalues could change the dynamic response, hopefully for the better.

Table 1. Comparison of Eigenvalues using Odd-Even Formulation

Mode	Morillo-Peters	Hsieh-Peters	% Difference
1	-	0.1718	-
2	1.0693	1.2817	19.9%
3	3.0633	3.2573	6.3%
4	5.4685	5.6414	3.2%
5	8.5160	8.7298	2.5%
6	11.5073	11.7648	2.2%
7	34.8999	36.0740	3.4%
8	51.0382	52.5394	2.9%

Following the eigenvalue analysis, we compare the mode shapes for each mode against the Morillo-Peters model. In order to calculate the mode shapes, we utilize the mode shape function:

$$\overline{\upsilon} = \sum_{m,n} \alpha_n^m \overline{P}_n^m(\nu)\,\overline{Q}_n^m(i\eta)\cos(m\overline{\psi}) \qquad \textbf{(3)}$$

where α_n^m represents the modes, $\overline{P}_n^m(\nu)$ and $\overline{Q}_n^m(i\eta)$ represents normalized associated Legendre functions of the first and second kind (Eqs. (4) and (5)) and $\overline{\psi}$ is the azimuth angle.

$$\overline{P}_n^m = (-1)^m \frac{P_n^m(\nu)}{\rho_n^m} \qquad \textbf{(4)}$$

$$\overline{Q}_n^m = \frac{Q_n^m(i\eta)}{Q_n^m(i0)} \qquad \textbf{(5)}$$

where ρ_n^m is defined as:

$$\left(\rho_n^m\right)^2 = \int_0^1 \left[P_n^m(\nu)\right]^2 d\nu = \frac{1}{2n+1}\frac{(n+m)!}{(n-m)!} \qquad \textbf{(6)}$$

and $Q_n^m(i0)$ is defined as:

$$Q_n^m(i0) = \begin{cases} \dfrac{\pi}{2}(-1)^{m+n+1}(i)^{n+1}\dfrac{(n+m-1)!!}{(n-m)!!} & n+m=even \\ (-1)^{m+n+1}(i)^{n+1}\dfrac{(n+m-1)!!}{(n-m)!!} & n+m=odd \end{cases} \qquad \textbf{(7)}$$

Since we are only looking at axial flow, the azimuth angle is equal to zero. In order to obtain a better correlation between the two models, we normalized the mode shapes. The modes show that the low-damping (slow) mode is dominated by the new basis function. Figs. 3 to 6 show that the higher modes are not changed by the new basis function.

On-Off Formulation

The On-Off formulation was briefly introduced in Jorge Morillo's doctoral thesis. The On-Off formulation is a change of variable that separates the odd and even terms in the Morillo-Peters model into on-disk and off-disk modes. The change in variable for the equation of motion is defined as:

$$\begin{Bmatrix} \{\hat{a}_n^m\}_o \\ \{\hat{a}_n^m\}_e \end{Bmatrix} = \begin{bmatrix} [I] & -[U] \\ [0] & [I] \end{bmatrix} \begin{Bmatrix} \{\gamma_n^m\} \\ \{\delta_n^m\} \end{Bmatrix} \qquad \textbf{(8)}$$

Substituting this relationship into the original equation of motion, and we obtain the equation using the On-Off formulation.

$$\begin{bmatrix} [M]_{on,on} & 0 \\ 0 & [M]_{off,off} \end{bmatrix} \begin{Bmatrix} \{\ddot{\gamma}_n^m\} \\ \{\ddot{\delta}_n^m\} \end{Bmatrix} + \begin{bmatrix} [D]_{on,on} & [D]_{on,off} \\ [D]_{off,on} & [D]_{off,off} \end{bmatrix} \begin{Bmatrix} \gamma_n^m \\ \delta_n^m \end{Bmatrix} = \begin{bmatrix} [F]_{on,on} & [F]_{on,off} \\ [F]_{off,on} & [F]_{off,off} \end{bmatrix} \begin{Bmatrix} \{\tau_n^m\}_o \\ \{\tau_n^m\}_e \end{Bmatrix} \quad \textbf{(9)}$$

The advantage for the On-Off formulation is that the mass matrix uncouples into "On" modes and "Off" modes. Theoretically, this method should simplify the analysis. However Morillo and Peters did not further investigate the advantage of the On-Off formulation.

Similarly to the Odd-Even formulation, the original On-Off formulation did not include the zero-zero term in the mass matrix. We used the same logic for the Odd-Even formulation and derived an approximate solution for the zero-zero term in the on-off mass matrix. The resulting equation for the zero-zero term as N approaches infinity for the On-Off formulation is:

$$\left[M_{00}^{00} \right]_{off,off} = \frac{4}{\pi^2} \sum_{n=1}^{N} \frac{1}{n} \quad \textbf{(10)}$$

Similar to the Odd-Even formulation, we compare the eigenvalues of the On-Off formulation to the values obtained using the Morillo-Peters and Hsieh-Peters model. The results are tabulated in Table 2. The initial result from the eigenvalue analysis shows that the On-Off values are not matching accordingly to the Odd-Even formulations. For the On-Off formulation, we introduce a zero mode to the system. This zero mode is not the low frequency mode already seen in the odd-even due to the infinite kinetic energy. This new zero-frequency mode appears to be a spurious mode introduced by the change of variable. Because of the zero mode, the eigenvalues are shifted up, thus we also end up losing the last mode. Some of the eigenvalues do not correspond accordingly to the eigenvalues from the Odd-Even formulation. In order to obtain a better understanding on the validity of the On-Off formulation, it is necessary to compare the mode shapes of such model to the Odd-Even model.

Table 2. Comparison of Eigenvalues for Morillo-Peters, Hsieh-Peters and On-Off model

Mode	Morillo-Peters	Hsieh-Peters	On-Off
0	-	-	0.0304
1	-	0.1718	0.2204
2	1.0693	1.2817	1.1994
3	3.0633	3.2573	2.5229
4	5.4685	5.6414	5.2540
5	8.5160	8.7298	8.4786
6	11.5073	11.7648	13.4100
7	34.8999	36.0740	45.0754
8	51.0382	52.5394	-

Following the eigenvalue analysis, we compare the mode shapes for each mode against the Morillo-Peters model. In order to calculate the mode shapes, we utilize the mode shape function defined in terms of the Odd (α_o) and Even (α_e) modes.

$$\bar{\upsilon} = \left[\left(\bar{P}_o(\nu) \bar{Q}_o(i\eta) \right)^T \middle| \left(\bar{P}_e(\nu) \bar{Q}_e(i\eta) \right)^T \right] \begin{Bmatrix} \alpha_o \\ \alpha_e \end{Bmatrix} \quad \textbf{(11)}$$

Since we used a coordinate transformation matrix to obtain the On-Off formulation, we can use the transformation matrix to obtain a mode shape function in terms of On and Off modes by making the substitution from Eq. (12) into Eq. (11), and we obtain the mode shape function defined in terms of On (γ) and Off (δ) modes.

$$\begin{Bmatrix} \gamma \\ \delta \end{Bmatrix} = \begin{bmatrix} I & U \\ 0 & I \end{bmatrix} \begin{Bmatrix} \alpha_o \\ \alpha_e \end{Bmatrix} \quad \textbf{(12)}$$

The resulting mode shape function in terms of On and Off modes is defined as:

$$\bar{\upsilon} = \left(\bar{P}_o(\nu) \bar{Q}_o(i\eta) \right)^T (\gamma - U\delta) + \left(\bar{P}_e(\nu) \bar{Q}_e(i\eta) \right)^T \delta \quad \textbf{(13)}$$

where U is defined as:

$$U_{jn}^m = \sqrt{\frac{H_n^m}{H_j^m}} \frac{\sqrt{(2j+1)(2n+1)}}{(j+n+1)(j-n)} (-1)^{\frac{j+n-2m-1}{2}} \quad \textbf{(14)}$$

for only $j + m = odd$ and $n + m = even$ terms including the $n = m$ case.

From Figs. 3 to 6, we concluded that the On-Off formulation is not an effective formulation that captures all the details of the flow field. At the lower modes, the correlation between the On-Off formulation and the Hsieh-Peters model result in a significant amount of error. Also, since the On-Off formulation shifts the eigenvalues, we have an extra mode with an eigenvalue almost equal to zero. Also, for modes one and two, shown in Figs 4 and 5, it

seems that the "On" mode from mode one is interchanging with the "On" mode from mode two. However, as we go to a higher mode, the mode shapes do tend to correlate nicely, as shown in Fig. 6.

Frequency Response

Following the mode shape analysis, the next step is to look at the frequency response of the Hsieh-Peters model and how it correlates to the Morillo-Peters model. However, in order to have an exact baseline, we also compare both solutions to the convolution integral. This preliminary analysis explores the zero frequency and critical frequency response for axial flow. The critical frequencies chosen for $n > m$ are taken from the work of Morillo, and are the frequencies for which Morillo and He models have the largest discrepancies. Critical frequencies for $m = n$ are chosen so as to roughly extrapolate from the $n > m$ values.

Table 3. Critical Frequencies for Individual Pressure Distribution

n \ m	0	1	2	3
0	1.2	2.3	5.0	10.1
1		4.0	7.3	12.0
2			8.0	14.0
3				16.0

For the frequency response for the dynamic wake model, the momentum equation for axial flow is defined as:

$$[M]\left\{\overset{*}{\hat{a}}{}_n^m\right\}+[D]\left\{\hat{a}_n^m\right\}=[D]\left\{\tau_n^m\right\} \qquad \textbf{(15)}$$

In order to solve for the frequency response, we assume a simple harmonic solution for the induced flow coefficient ($\hat{a}_n^m$) and the pressure expansion coefficient (τ_n^m), and substitute this form into Eq. (15) to obtain a general solution with respect to the forcing frequency.

$$\left\{\overline{a}_n^m\right\}[i\omega[M]+[D]]=[D]\overline{\tau}_n^m \qquad \textbf{(16)}$$

Solving for the complex modulus of the induced flow coefficient, we obtain:

$$\left\{\overline{a}_n^m\right\}=[i\omega[M]+[D]]^{-1}[D]\overline{\tau}_n^m \qquad \textbf{(17)}$$

Now using the relationship from Eq. (17), we obtain the solution for the frequency response.

$$v_z=\sum_{n=m}^{\infty}\mathrm{Re}\left[\overline{a}_n^m\right]\overline{P}_n^m(\nu)\overline{Q}_n^m(i\eta)\cos(m\psi)\cos(\omega t) -\sum_{n=m}^{\infty}\mathrm{Im}\left[\overline{a}_n^m\right]\overline{P}_n^m(\nu)\overline{Q}_n^m(i\eta)\cos(m\psi)\sin(\omega t) \qquad \textbf{(18)}$$

We utilize the convolution integral for comparison for the Hsieh-Peters model. The convolution integral is expressed as the following for the real and imaginary component of axial flow with respect to the stream-wise direction ξ.

$$\mathrm{Re}\left[v_z(\xi_o)\right]=\int_{+\infty}^{\xi_o}\cos\left(\omega(\xi_o-\xi)\right)\left(-\Phi_n^{mc}\right)_{,z}d\xi \qquad \textbf{(19)}$$

$$\mathrm{Im}\left[v_z(\xi_o)\right]=\int_{+\infty}^{\xi_o}\sin\left(\omega(\xi_o-\xi)\right)\left(-\Phi_n^{mc}\right)_{,z}d\xi \qquad \textbf{(20)}$$

For axial flow, we integrate from infinity down to the rotor disk, which is $\xi_o = 0$. The pressure potential function is defined as:

$$\left(\Phi_n^{mc}\right)_{,z}= -\frac{1}{\nu^2+\eta^2}\left(\eta\left(1-\nu^2\right)\frac{\partial\Phi_n^{mc}}{\partial\nu}+\nu\left(1+\eta^2\right)\frac{\partial\Phi_n^{mc}}{\partial\eta}\right) \qquad \textbf{(21)}$$

The partial derivatives for the pressure potential function with respect to ν and η are expressed as functions of Legendre functions of the first and second kind.

$$\left(1-\nu^2\right)\frac{\partial\Phi_n^{mc}}{\partial\nu}= \left(\sqrt{\frac{(2n+1)\left(n^2-m^2\right)}{(2n-1)}}\overline{P}_{n-1}^m(\nu)-n\nu\overline{P}_n^m(\nu)\right)\overline{Q}_n^m(i\eta) \qquad \textbf{(22)}$$

$$\left(1+\eta^2\right)\frac{\partial\Phi_n^{mc}}{\partial\eta}= \overline{P}_n^m(\nu)\left(-\frac{1}{K_n^m}\overline{Q}_{n+1}^m(i\eta)-(n+1)\eta\overline{Q}_n^m(i\eta)\right) \qquad \textbf{(23)}$$

where the Legendre constant, K_n^m is defined as:

$$K_n^m=\left(\frac{2}{\pi}\right)H_n^m \qquad \textbf{(24)}$$

for $n + m = odd$ and

$$K_n^m=\left(\frac{\pi}{2}\right)H_n^m \qquad \textbf{(25)}$$

for $n + m = even$. However, Eqs. (22) and (23) do not hold true when $m = n = 0$. Therefore, for this special case, the pressure potential function is described as:

$$\left(\Phi_0^0\right)_{,z}=-\frac{2}{\pi}\frac{\nu}{\nu^2+\eta^2} \qquad \textbf{(26)}$$

The resulting plots for the Hsieh-Peters model, shown in Figs. 7 to 16, correlate almost exactly to the solution of the Morillo-Peters model (when $n > m$) and the convolution integral for all m, n. In order to obtain a good correlation for the zero frequency response, we used the same number of odd

and even terms for the comparison to the Morillo-Peters model, and we used for the critical frequency response one more even term due to the extra row and column. The convolution integral correlation is actually not exact, due to the stream-wise step used in the integration. Further analysis and computing power will be needed to prove a better correlation between the Hsieh-Peters and convolution solutions. However, for $\omega = 0$ there is a closed-form exact solution; and that agrees exactly with our new model.

Conclusions

From the preliminary analysis of the newly formulated Hsieh-Peters model, the results are very promising. The basis for this research is to improve the conditioning of the matrices and the slow convergence from the Morillo-Peters model by including the infinite (zero-zero) term in the mass and damping matrix. For the Odd-Even formulation, we obtained excellent correlation with the Morillo-Peters model, both with the eigenvalue analysis and the mode shape plots. Because we add an extra row and column, we introduced a new mode to the system that represents the infinite kinetic energy term. However for the On-Off formulation, we could not obtain an acceptable correlation. This error could be attributed to the derivation of the equation for the "off-off" modes, or it may mean that it is not possible to fully separate the "on" mode from the "off" mode. At this point, we are abandoning the On-Off approach.

Following the mode shape analysis, we performed frequency response analysis to compare the new solution to the current solution obtained by Morillo and the convolution integral. We obtained excellent correlation with the Morillo-Peters model, however our correlation with the convolution did not match at the blade tip. This is due to the stream-wise step size selected for the preliminary analysis.

So far, we have only looked at one component of the frequency response in axial flow. The next step is to look at the two other components, radial and azimuthal, and perform zero frequency and critical frequency responses. Also, when we correlate our solution to the solution obtained from the convolution integral, we will need to use a smaller stream-wise step size in order to correct the discrepancy at the blade tip.

References

1. Pitt, D.M. and Peters, D.A., "Theoretical Prediction of Dynamic-Inflow Derivatives," *Vertica*, Vol. 5, No. 1, March 1981, pp. 21-34.
2. Peters, D.A., Boyd, D.D. and He, C.J., "A Finite-State Induced-Flow Model for Rotors in Hover and Forward Flight," *Journal of American Helicopter Society*, Vol. 34, No. 4, October 1989, pp. 5-17.
3. Morillo, J. and Peters, D.A., "Helicopter Rotor Dynamics Inflow Modeling for Maneuvering Flight," *Journal of Aircraft*, Vol. 39, No. 5, Sept-Oct 2002, pp. 731-738.
4. Peters, D.A., Morillo J. and Nelson A.M, "New Developments in Dynamic Wake Modeling for Dynamic Applications," *Journal of American Helicopter Society*, Vol. 48, No. 2, April 2003, pp. 120-127.
5. Yu, K. and Peters, D.A., "State-Space Inflow Modeling for Lifting Rotors with Mass Injection," *The Aeronautical Journal of the Royal Aeronautical Society*, Vol. 108, No. 1085, July 2004, pp. 333-344.

Acknowledgements

The work in this paper was sponsored through the National Rotorcraft Technology Center through the Georgia Tech/ Washington University Center of Excellence for Rotorcraft Technology, and by NASA Grant No. NAG 2-1457, Chee Tung, Technical Monitor.

Figures

Conditioning Plots

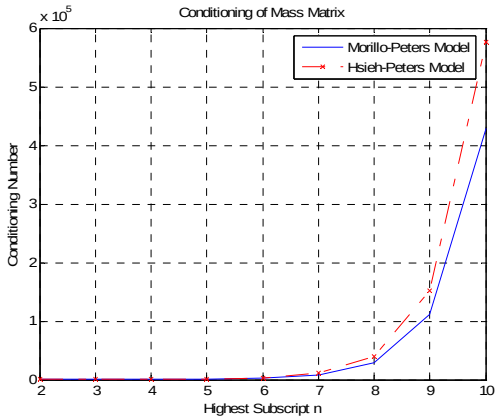

Figure 1. Comparison of the conditioning number for the mass matrix

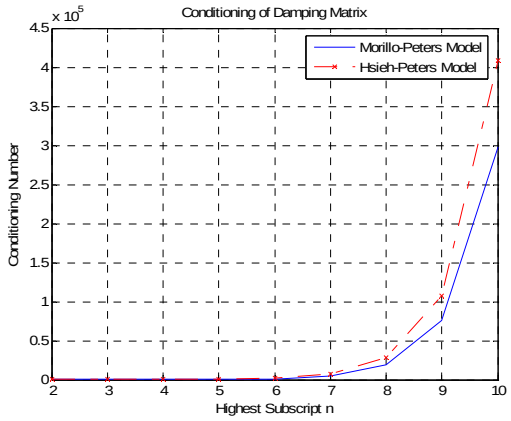

Figure 2. Comparison of the condition number for the damping matrix

Mode shapes Plots

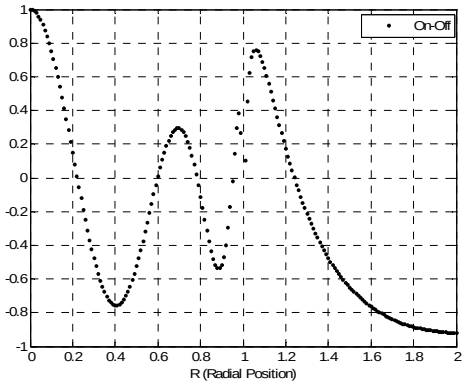

Figure 3. Mode 0 plot using On-Off Formulation

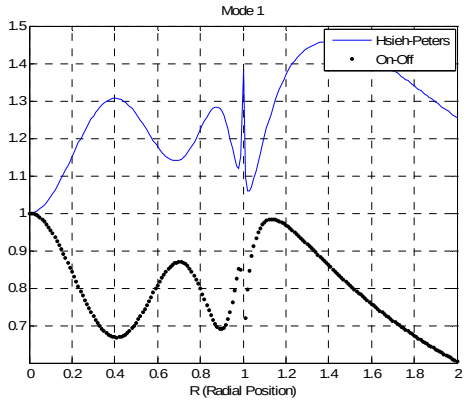

Figure 4. Mode 1 plot correlation between Hsieh-Peters model (solid line) and the On-Off formulation (dotted)

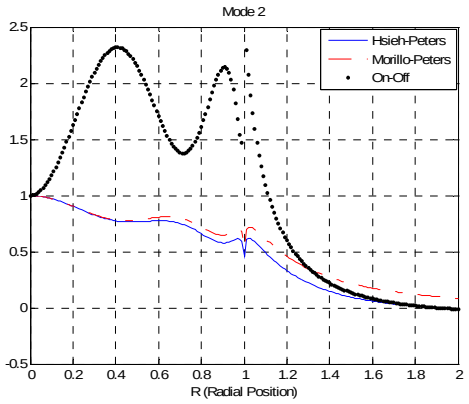

Figure 5. Mode 2 plot correlation between Hsieh-Peters model (solid line), Morillo-Peters model (dash line) and On-Off formulation (dotted)

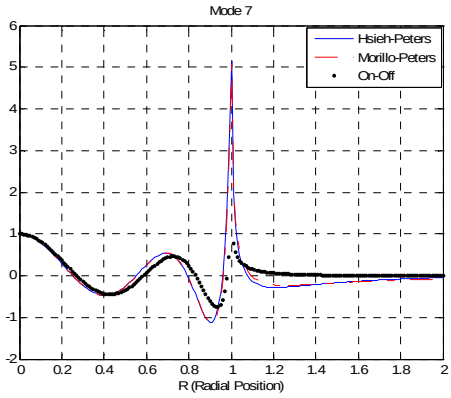

Figure 6. Mode 7 plot correlation between Hsieh-Peters model (solid line), Morillo-Peters model (dash line) and On-Off formulation (dotted)

Zero Frequency Response Plots

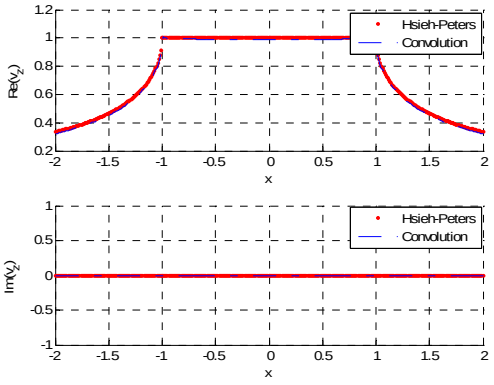

Figure 7. Zero frequency response plot for $\omega = 0, P = \Phi_0^0, \chi = 0, \psi = 0^o, 180^o$ and $z = 0$ for 4 odd terms and 4 even terms compared to the solution from the convolution integral

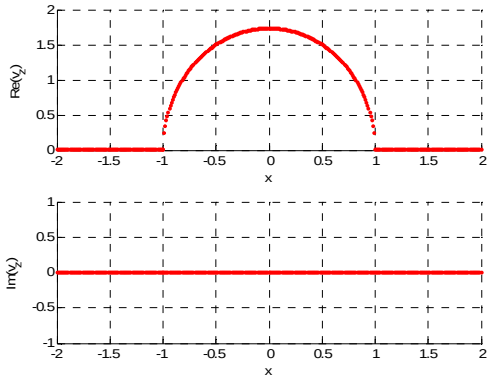

Figure 8. Zero frequency response plot for $\omega = 0, P = \Phi_1^0, \chi = 0, \psi = 0^o, 180^o$ and $z = 0$ for 4 odd terms and 4 even terms

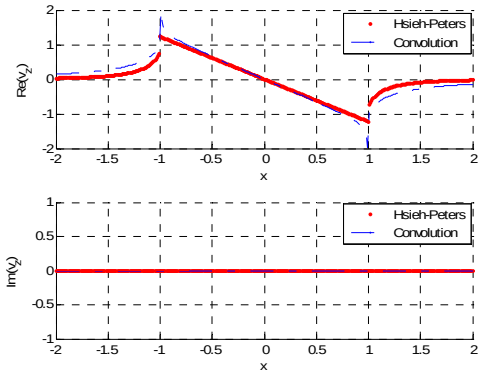

Figure 9. Zero frequency response plot for $\omega = 0, P = \Phi_1^1, \chi = 0, \psi = 0^o, 180^o$ and $z = 0$ for 4 odd terms and 4 even terms compared to the solution from the convolution integral

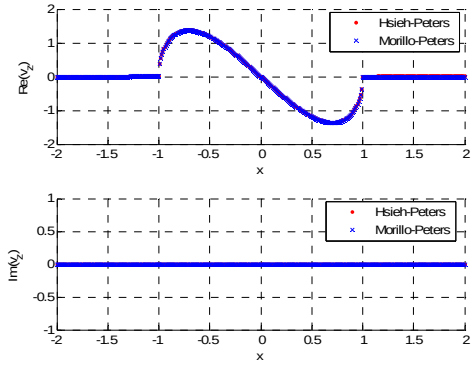

Figure 10. Zero frequency response plot for $\omega = 0, P = \Phi_2^1, \chi = 0, \psi = 0^o, 180^o$ and $z = 0$ for 4 odd terms and 4 even terms compared to the solution Morillo-Peters model

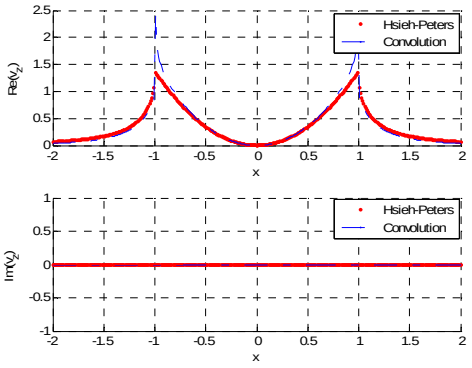

Figure 11. Zero frequency response plot for $\omega = 0, P = \Phi_2^2, \chi = 0, \psi = 0^o, 180^o$ and $z = 0$ for 4 odd terms and 4 even terms compared to the solution from the convolution integral

Critical Frequency Response Plots

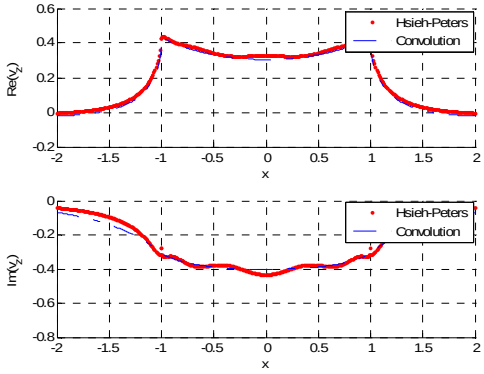

Figure 12. Critical frequency response plot for $\omega = 1.2, P = \Phi_0^0, \chi = 0, \psi = 0^o, 180^o$ and $z = 0$ for 4 odd terms and 4 even terms compared to the solution from the convolution integral

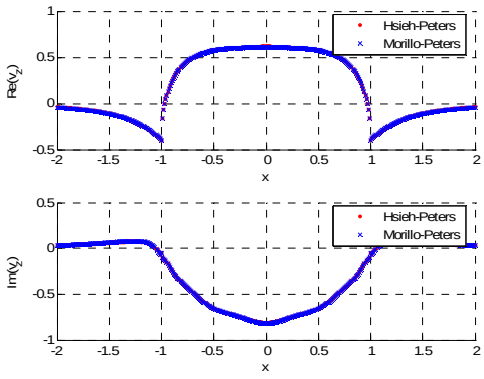

Figure 13. Critical frequency response plot for $\omega = 2.3, P = \Phi_1^0, \chi = 0, \psi = 0^o, 180^o$ and $z = 0$ for 5 odd terms and 6 even terms compared to the solution from Morillo-Peters for 5 odd terms and 5 even terms

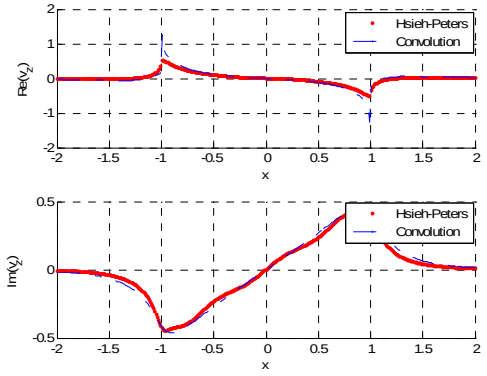

Figure 14. Critical frequency response plot for $\omega = 4, P = \Phi_1^1, \chi = 0, \psi = 0^o, 180^o$ and $z = 0$ for 5 odd terms and 6 even terms compared to the solution from the convolution integral

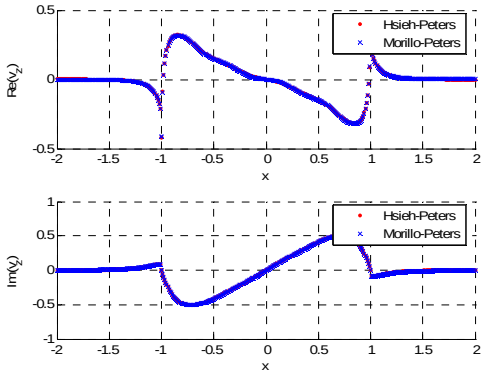

Figure 15. Critical frequency response plot for $\omega = 7.3, P = \Phi_2^1, \chi = 0, \psi = 0^o, 180^o$ and $z = 0$ for 5 odd terms and 6 even terms compared to the solution from Morillo-Peters for 5 odd terms and 5 even terms

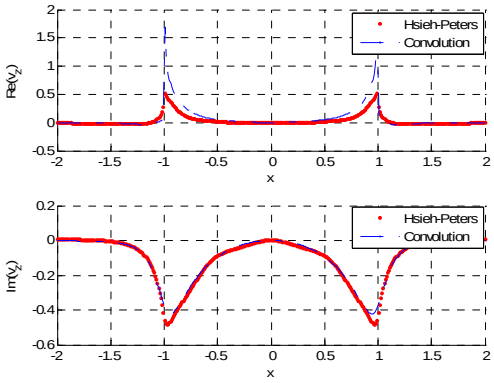

Figure 16. Critical frequency response plot for $\omega = 8, P = \Phi_2^2, \chi = 0, \psi = 0^o, 180^o$ and $z = 0$ for 5 odd terms and 6 even terms compared to the solution from the convolution integral